Adam Pacławski ⓘ
Jakub Szlęk ⓘ
Aleksander Mendyk ⓘ

COMPUTATIONAL INTELLIGENCE FOR PREDICTING BIOLOGICAL EFFECTS OF DRUG ABSORPTION IN LUNGS

Abstract

Recently, the lungs have been extensively examined as a route for delivering drugs (active pharmaceutical ingredients, APIs) into the bloodstream; this is mainly due to the possibility of the noninvasive administration of macromolecules such as proteins and peptides. The absorption mechanisms of chemical compounds in the lungs are still not fully understood, which makes pulmonary formulation composition development challenging. This manuscript presents the development of an empirical model capable of predicting the excipients' influence on the absorption of drugs in the lungs. Due to the complexity of the problem and the not-fully-understood mechanisms of absorption, computational intelligence tools were applied. As a result, a mathematical formula was established and analyzed. The normalized root-mean-squared error (NRMSE) and R^2 of the model were 4.57%, and 0.83, respectively. The presented approach is beneficial both practically by developing an in silico predictive model and theoretically by gaining knowledge of the influence of APIs and excipient structure on absorption in the lungs.

1. Introduction

Active pharmaceutical ingredients (APIs) have been delivered through the respiratory tract for therapeutic and recreational purposes for at least 4000 years. The application of medicinal aerosols has evolved from inhaling smoke or steam from the burnt and boiled parts of plants. Further development led to the development of efficient delivery systems to treat local respiratory tract diseases [41]. Finally, the lungs have recently been considered as a noninvasive route to deliver APIs directly to the bloodstream for macromolecules such as peptides and proteins [2]. The pulmonary route of administering macromolecular APIs has been extensively examined for insulin [43], parathyroid hormones [38], calcitonin, thyroid-stimulating hormone, follicle-stimulating hormone, growth hormone, immunoglobulins, and cyclosporine [1]. The bioavailability of macromolecules administered into the lungs is related to their large surface area, thin alveolar epithelium, reduced mucociliary clearance, and low enzymatic activity. However, the complex anatomical structure of respiratory tracts and still-not-fully-understood mechanisms of chemical compound absorption cause pulmonary formulation development to be challenging [33]. Deposition in the lungs is a topic of particle design and delivery system development, whereas drug absorption is examined by performing tests on animals or cell cultures [10, 48].

API absorption from the respiratory tract depends on the dynamic interaction of several factors, including the dose, used excipients, and physicochemical properties of the drug (such as molecular weight, lipophilicity, solubility, and charge). Excipients are a group of inactive chemical compounds which enable obtaining proper dosage form, guarantee its stability during storage and bioavailability after drug administration [20]. The mechanisms of chemical compound absorption in the lungs include passive diffusion, receptor-mediated transport, and transcytosis [30]. Additionally, absorption can be modified by drug administration with excipients called absorption enhancers; however, the mechanisms of permeability enhancement are not fully understood for the most part [17].

The manuscript presents the development of an empirical model that, when based on formulation composition and chemical descriptors, is capable of predicting the excipients' influence on the absorption of an API in the lungs. The given results include database construction by encoding the quantitative and qualitative compositions of the formulations, the selection of critical variables, the builds of predictive models, and their analysis. The research goals are as follows:

1. Create a database numerically representing a given problem and select critical variables.
2. Build an empirical model capable of expressing a given problem by applying different computational tools.
3. Analyze constructed model in a way to search how changes in variables influence predicted drug bioavailability.

The following section "Related work" briefly presents recent research in the field of drug absorption by the lungs after its administration (including laboratory work and a numerical analysis) as well as the computational tools used in the research topic. Section 3 ("Methods") contains a description of the database and computational tools, including the settings applied in the work. The results of the feature selection and the best-performing models are presented in Section 4 ("Results"), whereas a final model analysis with a scientific discussion is included in Section 5 ("Model-based problem analysis and discussion"). The manuscript ends with the "Conclusions" section, where we indicate how the presented approach fits in the current trends of applying AI tools in the pharmaceutical industry, and clinical practice.

2. Related work

The lungs are considered to be a route for the administration of active substances intended to treat diseases locally (e.g., asthma, infections) as well as systemic diseases (e.g., diabetes). Independent of the goal of an API's administration to the lungs, its absorption is critical for patient safety and therapy effectiveness. In the case of locally acting drugs, the lower absorption results in less-frequent systemic side effects. On the other side, the high bioavailability of administered drug reduces the total dose and local side effects like irritation or immune system response. The absorption, distribution, and pharmacodynamic effects of inhaled pharmaceuticals are mainly assessed using *in vivo* animal models. The animal can be anesthetized or conscious, whereas the formulations are delivered by inhalation or insufflation into the lungs with or without surgical intervention. Besides the above, cell-based *in vitro* models are applied to study the uptake, transport, and metabolism of drugs from the lungs. Over the past few decades, cell culture models have received increasing acceptability due to their cost reduction and fast throughput. Drug absorption is also examined using an *ex vivo* lung model [33]. Nowadays, the development and optimization of pulmonary formulation is still mainly based on the trial-and-error approach. This is mainly due to the not-fully-understood mechanisms of drug absorption by the lungs as well as the factors that influence them. So far, a few mechanisms of drug transport from the lungs have been proposed; i.e., transport through the pores in the membrane, transport through intracellular tight junctions, vesicular transport, active transport, and drainage to the lymphatics. All of them are grouped as paracellular or transcellular transport [19]. Apart from this, other factors affecting bioavailability are still being investigated. For example, Price et al. used an isolated perfused mouse lung (IPML) model to analyze the impact of P-glycoprotein on the absorption of 18 chemical compounds that were recognized as P-gp substrates. Two types of mice were used in the *in vivo* study; i.e., with active P-gp transporter (Mdr1a/1b (+/+)) and with knocked-out P-gp transporter (Mdr1a/1b (-/-)). The compounds were divided into two groups based on their affinity to the P-gp. Next, 13 chemical descriptors were calculated, and an orthogonal partial least squares (oPLS) model was developed to classify the molecules. The authors concluded that the absorption of polar compounds character-

ized by low phospholipid membrane affinity and low transmembrane movement was not affected by P-gp. The classification model ($R^2 = 0.59$), with its possible application as a screening tool for new molecules and the possibility of its absorption affected by P-gp activity, was presented. The predictions of the model were not quantitative, and its application in terms of binary or ternary formulations was limited [39]. Wang et al. examined the absorption of four proteins: salmon calcitonin (sCT), insulin (INS), recombinant hirudin (rHAV2), and the recombinant human growth hormone (rhGH) through a human cultured alveolar A549 cell monolayer. As a result, the authors proposed that the examined proteins are absorbed by a passive diffusion mechanism. The apparent permeability coefficient (Papp) was significantly lower only for rhGH when compared to the other compounds, which were explained by the rhGH's higher molecular weight (MW). A quantitative relationship was not proposed due to insufficient data [50]. Tronde et al. analyzed the pulmonary absorption of nine low-molecular-weight drugs (atenolol, budesonide, enalaprilat, enalapril, formoterol, losartan, metoprolol, propranolol, and terbutaline) and one high-molecular-weight membrane permeability marker compound (FITC-dextran, MW=10k Da). The experiments were performed using an isolated, perfused, and ventilated rat lung model (IPL). All of the analyzed compounds were characterized by nine descriptors and the apparent permeability of Caco-2 cell monolayers. Based on the obtained data, a partial least squares (PLS) model for absorption rate was developed ($R^2 = 0.78$). It was found that drug absorption was negatively correlated to the molecular polar surface area and positively correlated to the lipophilicity (cLogD) [49]. Erikson et al. studied pulmonary permeability and tissue retention for ten drugs using an isolated perfused rat lung (IPL). The collected data was applied to develop a compartmental *in silico* model of pulmonary permeability and tissue retention of the analyzed chemical compounds. It was established that pulmonary permeability and the intrinsic permeability of Caco-2 cell monolayers is highly correlated ($R^2 = 0.76$). The authors also examined the possible influence of ethanol to salbutamol and tiotropium absorption. It was found that using ethanol instead of water as an excipient resulted in a higher intake of tiotropium but did not affect the salbutamol. A further investigation in such a direction was not employed [11]. Edwards et al. developed a model to recognize the influence of the physicochemical properties of APIs on pulmonary absorption. The experimental data included 98 chemical compounds with molecular weights ranging from 177 to 842 Da. The absorption was tested using the isolated perfused respiring rat lung, and the chemical structures were encoded by molecular descriptors and additional *in silico* ADME related endpoints. The model was developed using an orthogonal partial least squares regression (oPLS) preceded by a principal component analysis (PCA). The model was tested on nine additional compounds, resulting in 65% that were correctly categorized [10]. Bäckman et al. presented a comprehensive review of mechanistic models of the local exposure on inhaled drugs. In summary, it was pointed out that there is a lack of generally recognized commercially available computational models incorporating the mechanistic modeling of regional lung particle deposition and drug disposition processes to simulate free tissue drug con-

centration. Moreover such a state is most likely related to the lack of proper data, not-fully-established and reliable bio-relevant methods to examine drug disposition after inhalation, and the lack of a full understanding of absorption mechanisms [3].

To the best of the authors' knowledge, there is no available computational model predicting the influence of excipients on API absorption in the lungs. Due to the complexity of the analyzed problem, the still-not-fully-understood mechanisms of drug absorption, and their modification by excipients, an empirical approach was proposed. A set of computational intelligence techniques including random forest, rule-based systems, neural networks, and genetic programming (GP) were applied to develop a predictive model. As a result, a mathematical formula was created with GP methods providing the opportunity to calculate *in silico* the effect of the excipient on the API absorption in the lungs.

3. Methods

The general work procedure consisted of database construction, crucial variable selection, model development, testing, and finally model analysis in order to assess the input variables' influence on the output variable. A scheme presenting the major steps of the work is presented in Figure 1.
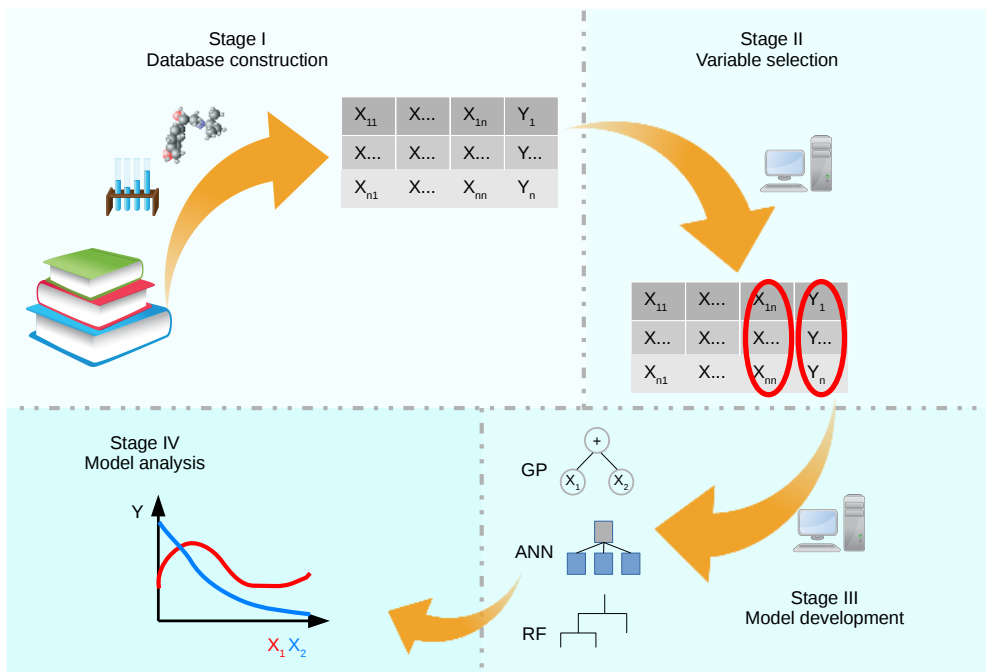

Figure 1. General scheme of work

3.1. Data set

The database was constructed based on the experimental data extracted from fourteen publications [9,16,18,22,25,26,28,29,31,34,36,44,52,53], where the influence of various excipients on API absorption in the lungs was examined. In brief, the literature data was arranged in a matrix, where the columns represent the features and the rows represent the instances of the formulations (Fig. 2).
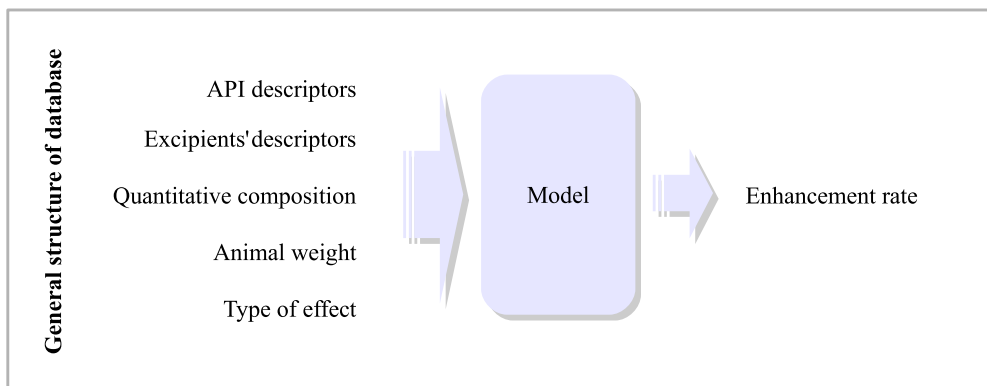

Figure 2. General structure of database and created models.

Initially, the input vector consisted of six inputs characterizing the formulation and assay. To diversify the input vector, chemical descriptors characterizing the APIs and excipients were incorporated in the database. There were 33 and 11 different excipients and APIs, respectively. The range of the molecular weights for the APIs was from 354 Da to 19,102 Da, whereas the excipients' MW differed from 88 Da to 6849 Da. In order to calculate the molecular descriptors, the chemical structures of the molecules were downloaded from PubChem [21]. The proteins and peptides were modeled using the Swiss-Model server [5] and downloaded as PDB files prior to usage. Eventually, Mordred software [32] was used to obtain the chemical descriptors of all molecules. A Mordred-descriptor calculator was used due to its ease of installation and usage, high calculation speed, and large number of calculated molecular descriptors. The calculated molecular descriptors of the APIs and excipients were included in the database, where each molecule was represented by 1826 chemical descriptors. In summary, the independent variables were grouped into four categories: 1) API chemical descriptors, 2) first excipient chemical descriptors, 3) second excipient chemical descriptors, 4) experimental conditions, including API dose [μg], Enhancer 1 dose [μg], Enhancer 2 dose [μg], formulation type (1 = powder, 2 = liquid form), animal weight [g], and type of effect (1 = pharmacokinetic, 2 = pharmacodynamic). The enhancement ratio (ER) was a single output variable representing a modification of an API's absorption after its administration with an excipient.

The general formula for ER calculation is given by Equation 1.

$$ER = \frac{PK/PD_1}{PK/PD_0},$$ (1)

where ER – enhancement ratio, PK/PD_1 – pharmacokinetic or pharmacodynamic effect with excipient, PK/PD_0 – pharmacokinetic or pharmacodynamic effect without excipient.

When the pharmacokinetic (PK) data was available, the ER was calculated as a quotient of the area under the plasma drug concentration-time curve (AUC) of a formulation with an excipient and a control sample without an excipient. In the case of the pharmacodynamic effect measurement (like blood glucose levels after insulin administration), the ER was calculated as a quotient of an area above the plasma glucose level-time curve (AAC) of a formulation with an excipient and a control sample without an excipient. Therefore, in both cases, the ER is a dimensionless measure for the enhancer effect of API absorption in the lungs.

Afterwards, the raw database was preprocessed in order to remove inputs with zero variance and inputs with non-numerical values. In total, the database was composed of 134 records encoded with 4026 independent variables and 1 dependent variable, which was the enhancement ratio (ER). The complete database is attached as supplementary material to the manuscript (S1). Prior to feature selection, the database was split into ten pairs of training-testing sets according to the 10-fold cross-validation scheme (later in the text and tables, this will be noted as 10-cv).

3.2. Feature selection

The aim of the feature selection was to reduce the number of inputs in the database before the modeling process. The independent variable reduction was performed in order to simplify the developed models, to find the most important variables, and to save time and computational resources. In order to efficiently implement a model selection scheme, a variable selection was done. This limited the complexity level of the developed models. The feature selection was performed by the *fscaret* package [45] for the *R* environment [8]. The package was chosen due to its vast number of available models for feature-ranking creation, ease of control, and its good results from earlier research [45, 46, 51]. At the moment, *fscaret* includes various feature--ranking algorithms, which generate more than 100 models. The results are presented as a ranking of variables, with a calculated importance value for each variable. The obtained feature rankings were closely examined, and the cut-off points were set in the place where variables had a ranking parameter of SUM% (internal measure) of 70, 85, 90, or 95%. Regarding applied methodology (two error functions, RMSE and MSE) an overall of eight input vectors were selected.

3.3. Model construction and analysis

The modeling was performed in two-steps. First, fast algorithms such as rule-based (*Cubist*), multilayer perceptron (*monmlp*, *h2o*), and random forest (RF) were applied

in order to select the best input vector. Next, the genetic programming (GP) was implemented to obtain the mathematical equations. The search for the optimal model and its architecture was performed under the criterion of the minimum generalization error calculated with the 10-cv approach.

The *Cubist* [24] package is the implementation of rule-based predictive decision trees proposed by Quinlan [40]. The developed models have linear equations at their terminate branches; therefore, it is easy to predict the numeric values. Both the maximum number of rules and maximum number of committees were set at 100. The extrapolation parameter was also set to 100. No data subsampling was employed.

A *Monmlp* (monotonic multilayer perceptron) [7] was used to take advantage of learning without back-propagation. The monotonicity feature was turned off. All models had two hidden layers, each one numbering from 2 to 20 nodes. The hidden layer had a hyperbolic tangent (tansig) transfer function, and the output layer had the linear function applied. Ensemble systems were employed, consisting of ten neural networks. The epoch was set from 50 to 1000. The "trials" parameter was set to 5 to avoid getting stuck in the local minima. The deep architectures were also trained. The term "deep architecture" refers to a neural network composed of multiple hidden layers with many neurons within each layer. Deep-learning neural networks are used to solve complex problems by introducing combinations of simpler solutions. Therefore, these systems can operate in real-world environments [47] and can be useful in fitting a solution to empirical data. In order to develop deep-learning models, the *h2o* package was utilized [23]. The numeric values were standardized by the default function implemented in the *h2o* package to have zero mean and unit variance. The hyperbolic tangent was used as an activation function. Because of the larger structure of neural networks, the epochs varied from 1000 to 10,000,000. The neural nets consisted of 2 to 8 hidden layers with 2 to 200 nodes per layer. Overall, more than 2000 architectures of neural networks were trained and tested.

RandomForest (RF) creates an ensemble of decision trees using random inputs. Package *randomForest* of the *R* environment was used [27]. During the model's development, the following parameters were used: the number of randomly selected variables at each split was between 1 and half the size of a vector (mtry); the maximum number of nodes was set between 10 and 500 (maxnodes); and the number of trees was set from 10 to 500 (ntree). For comparison reasons, linear regression models were also included (noted later in the text as lm).

Genetic programming (GP) allows for the creation of computer programs by emulating the evolution process observed in nature. Advantages of using GP is the possibility of developing a predictive model while an analyzed problem is not fully understood from a mechanistic point of view. Comparing to other computational tools like neural networks, the architecture of the solution is not specified at the beginning but is defined in the evolution process. The disadvantage of GP is the long computational time and power consumption, especially when the space of the variables is large [14]. GP methods were applied to develop the mathematical models using

the *rgp* [13] package of the *R* environment. *Rgp* is an example of a tree-based GP system in which individuals are represented as *R* expressions that can be directly evaluated in the *R* environment. In the computational work, two search-heuristic optimization algorithms were applied to find the optimal solution to a given problem: the generational evolutionary multi-objective optimization algorithm (EMOA), and the archive-based Pareto tournament EMOA, in which both are dependent on three criteria: the individual's age, fitness, and complexity. The genetic programming method was applied to the data sets with reduced numbers of inputs. The size of the chromosome, which is a representation of the maximum length of the equation, varied from 10 to 100. The population size was set to 300, and the modeling process was set to 90 million evolution steps divided into 300 stages.

The computational experiment was designed to develop multiple input single output (MISO) models, where the single output variable was a relative enhancement of the PK or PD effect related to adding excipient composition (ER). The models' performance was evaluated according to a tenfold cross validation by three goodness--of-fit measurements: the root-mean-squared error (RMSE – Equation 2), normalized root-mean-squared error (NRMSE – Equation 3), and coefficient of determination (R^2 – Equation 4). The NRMSE was calculated according to the output variable range, which was from 0.545 to 21.125.

$$RMSE = \sqrt{\frac{\sum_{i=1}^{n} (pred_i - obs_i)^2}{n}}, \qquad (2)$$

where obs_i and $pred_i$ are the observed and predicted values, respectively, i – the data record number, and n – the total number of records.

$$NRMSE = \frac{RMSE}{X_{max} - X_{min}} \cdot 100\%, \qquad (3)$$

where RMSE is the error calculated for the model, X_{max} – the maximum value of the observed results, and X_{min} – the minimum value of the observed results.

$$R^2 = \frac{\sum_{i=1}^{n} (pred_i - obs_{mean})^2}{\sum_{i=1}^{n} (obs_i - obs_{mean})^2}, \qquad (4)$$

where R^2 is the coefficient of determination, obs_i and $pred_i$ are the observed and predicted values, respectively, and obs_{mean} – the arithmetic mean of the observed values.

4. Results

The obtained database combines the results of API absorption in the lungs from both the pharmacokinetic and pharmacodynamic studies. Due to the nonlinear relationship between the drug concentration in the plasma and the pharmacodynamic effect, the latter is not linearly linked to the absorption modification by the excipients.

Therefore, the task to build a model able to predict the absorption ratio from the data not containing any direct methods of absorption measurement was complicated. However, we overcame the difficulties and managed to obtain a predictive model with satisfactory performance.

4.1. Feature selection and model development

According to the feature ranking created by *fscaret*, eight input vectors with reduced dimensions were selected. The new vectors contained between 25 and 45 independent variables. The computational work began with developing the models using a set of computational methods such as linear regression *lm*, *Cubist*, *randomForest*, *monmlp*, and *h2o*. The results of the models' performances according to the 10-cv scheme are presented in Table 1.

Table 1

Performance of models created with different computational methods: PP – database pre-processed by *fscaret* package; noPP – database not pre-processed by *fscaret* package; RMSE – variable ranking based on root-mean-squared error; MSE – variable ranking based on mean-squared error

	RMSE	R^2	NRMSE [%]	Variables vector
lm	1.62	0.41	7.87	noPP RMSE 35 inputs
Cubist	1.31	0.61	6.37	PP MSE 32 inputs
randomForest	1.44	0.39	6.92	noPP RMSE 35 inputs
monmlp	1.27	0.61	6.16	no PP MSE 45 inputs
h2o	1.26	0.60	6.12	no PP MSE 45 inputs

The linear regression model exhibited the highest error value – NRMSE = 7.87% and $R^2 = 0.41$. The best models (NRMSE above 6% and $R^2 = 0.60$) were obtained for the neural networks created with the *h2o* and *monmlp* packages. The neural network model trained by the *h2o* package was constructed with four hidden layers, where the first hidden layer contained five neurons, the second contained three neurons, and last two contained two neurons each. The model was trained for 10,000,000 iterations, and the hyperbolic tangent was used as an activation function for the hidden layers. Slightly worse results were obtained by the expert committee created with the *monmlp* package. The model was composed of 10 neural networks with 2 hidden layers, which were composed of 28 and 8 neurons, respectively. The model was trained by processing 50 iterations, whereas the trial parameter was set as 5. The rule-based systems and random forest models resulted in NRMSE errors equal to 6.37% and 6.92%, respectively. The model with the lowest NRMSE was created based on the input vector with 45 independent variables; therefore, it was selected for further computations with the application of a genetic programming (GP) framework. The 45-input vector was composed of 15 variables involving API's molecular descriptors, 26 of the excipient's molecular descriptors, 2 the formulation's quantitative composition, and

2 assay parameters (the body mass of the animal and the experimental conditions). A complete description of the variables is presented in Table 2.

Table 2

Input vector with 45 variables selected for further computations with genetic programming methods. Variables included in the final model (Equation 5) are in bold

Original input	Input name	Input description
328	API AATSC6c	centered Moreau-Broto autocorrelation of lag 6 weighted by Gasteiger charge
329	API AATSC7c	centered Moreau-Broto autocorrelation of lag 7 weighted by Gasteiger charge
406	API AATSC4p	averaged Moreau-Broto autocorrelation of lag 4 weighted by polarizability
437	**API MATS6d**	**Moran coefficient of lag 6 weighted by sigma electrons**
442	API MATS4s	Moran coefficient of lag 4 weighted by intrinsic state
469	API MATS3se	Moran coefficient of lag 3 weighted by Sanderson EN
755	API WPSA2	surface weighted charged partial positive surface area (version 2)
781	**API Xch-7dv**	**7-ordered Chi chain-weighted by valence electrons**
833	API Mse	mean of constitutional weighted by Sanderson EN
850	API DetourIndex	detour index
977	**API BIC4**	**4-ordered bonding information content**
1025	API Mor24	3D-MoRSE (distance = 24)
1217	API MOMI.X	moment of inertia (axis = X)
1218	API MOMI.Y	moment of inertia (axis = Y)
1335	API WPath	Wiener index
1476	Excipient AATS2d	averaged Moreau-Broto autocorrelation of lag 2 weighted by sigma electrons
1558	Excipient ATSC4c	centered Moreau-Broto autocorrelation of lag 4 weighted by gasteiger charge
1562	Excipient ATSC8c	centered Moreau-Broto autocorrelation of lag 8 weighted by gasteiger charge
1576	Excipient ATSC4d	centered Moreau-Broto autocorrelation of lag 4 weighted by sigma electrons
1579	Excipient ATSC7d	centered Moreau-Broto autocorrelation of lag 7 weighted by sigma electrons
1593	Excipient ATSC3Z	centered Moreau-Broto autocorrelation of lag 3 weighted by atomic number
1602	Excipient ATSC3m	centered Moreau-Broto autocorrelation of lag 3 weighted by mass
1616	Excipient ATSC8v	centered Moreau-Broto autocorrelation of lag 8 weighted by vdw volume

Table 2 (cont.)

Input vector with 45 variables selected for further computations with genetic programming methods. Variables included in the final model (Equation 5) are in bold

Original input	Input name	Input description
1619	Excipient ATSC2se	centered Moreau-Broto autocorrelation of lag 2 weighted by Sanderson EN
1639	Excipient ATSC4are	centered Moreau-Broto autocorrelation of lag 4 weighted by Allred-Rocow EN
1666	Excipient AATSC4c	averaged and centered Moreau-Broto autocorrelation of lag 4 weighted by Gasteiger charge
1716	Excipient AATSC6v	averaged and centered Moreau-Broto autocorrelation of lag 4 weighted by vdw volume
1765	Excipient MATS1dv	Moran coefficient of lag 1 weighted by valence electrons
1816	**Excipient MATS3pe**	**Moran coefficient of lag 3 weighted by Pauling EN**
1817	Excipient MATS4pe	Moran coefficient of lag 4 weighted by Pauling EN
2272	Excipient ETA epsilon 3	ETA epsilon (type: 3)
2350	Excipient Mor09	3D-MoRSE (distance = 9)
2351	Excipient Mor10	3D-MoRSE (distance = 10)
2447	**Excipient Mor10se**	**3D-MoRSE weighted by Sanderson EN (distance = 10)**
2448	Excipient Mor11se	3D-MoRSE weighted by Sanderson EN (distance = 11)
2469	Excipient Mor32se	3D-MoRSE weighted by Sanderson EN (distance = 32)
2475	Excipient Mor06p	3D-MoRSE weighted by polarizability (distance = 6)
2489	Excipient Mor20p	3D-MoRSE weighted by polarizability (distance = 20)
2641	Excipient JGI6	6-ordered mean topological charge
2642	Excipient JGI7	7-ordered mean topological charge
2644	**Excipient JGI9**	**9-ordered mean topological charge**
4021	API dose [μg]	The dose of API in μg
4022	**Excipient 1 dose [μg]**	**dose of enhancer in μg**
4025	Animal weight [g]	Body mass of animal on which absorption tests were performed
4026	Enhancement measurement	Type of effect: 1 = pharmacokinetic; 2 = pharmacodynamic
4027	Enhancement rate	Output

Genetic programming computations with the *rgp* package were performed using *symbolicRegression()* function and two evolution algorithms: the generational evolutionary multi-objective optimization algorithm, and the archive-based Pareto tournament multi-objective optimization algorithm. The model with the lowest NRMSE

is presented as a mathematical formula in Equation 5. It was developed using the Pareto tournament evolutionary algorithm, where the maximum chromosome size was set to 40. The population size was established as 300, and the model was evaluated after every 300,000 evolution steps, whereas the total number of steps was 45,000,000. The NRMSE of the model was 4.57%, and the R^2 was 0.83, which is a 25% improvement when compared to the best-obtained neural network.

$$ER = \sqrt{X_{11}} \cdot e^{2X_{41} \cdot e^{X_8} + 2X_{11} \cdot X_8 + e^{\frac{1}{2}X_4 \sqrt{C_1 \cdot X_{41}}}} \cdot \sqrt{X_{41} \cdot X_{43}} + e^{C_2 \cdot |X_{29}| \cdot X_{34}} \quad (5)$$

where C_1–C_2 are constants, X_4 – API MATS6d, X_8 – API Xch-7dv, X_{11} – API BIC4, X_{29} – Excipient MAT3pe, X_{34} – Excipient Mor10se, X_{41} – Excipient JGI9, X_{43} – Enhancer dose [μg], ER – Enhancement ratio.

The GP model for ER prediction requires seven input variables among which three are API descriptors, three are excipient descriptors and one indicates the enhancer amount in the formulation. To summarize, an additional reduction of the features was done by discarding 38 variables of the previously selected 45-input vector as a result of the models' evolution. The ER values observed and predicted by the model are presented in Figure 3.
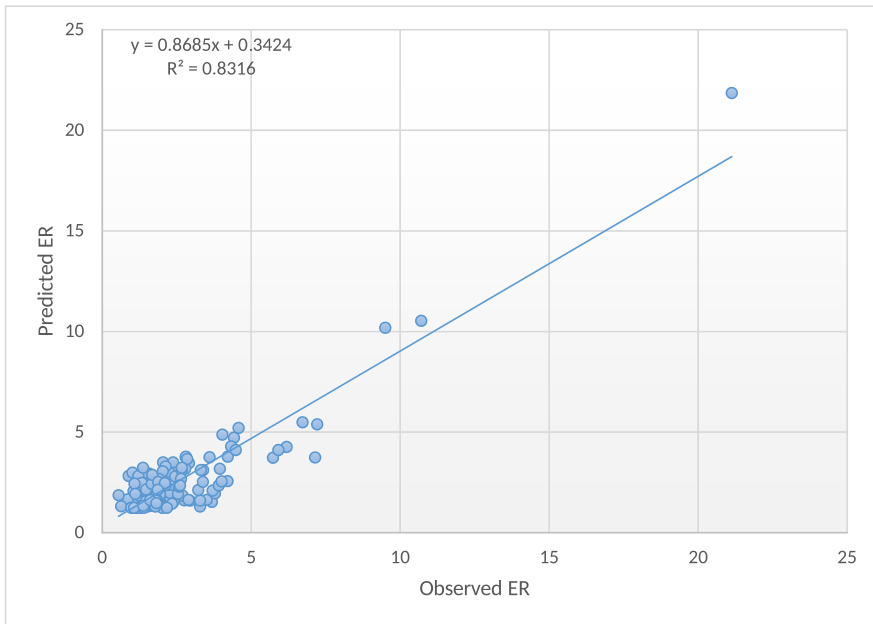

Figure 3. Predicted and observed values for GP model presented in Equation 5

The model presented in Equation 5 was also implemented in a simple computer application written in Python; it can be directly applied to calculate the excipients' influence on API absorption. The tool is available free of charge at the SourceForge website [37].

5. Model-based problem analysis and discussion

The best-performing model presented in Equation 5 was analyzed to discover the relationships between the variables in the analyzed problem. The influence of the input factors on the predicted ER values was analyzed visually on three-dimensional plots. It seems that, from the seven inputs included in Equation 5, the most significant are the enhancer's dose, the excipient's 9-ordered mean topological charge (Excipient's JGI9), the 7-ordered Chi chain-weighted by valence electrons (API Xch-7dv), and the Moran coefficient of lag 3 weighted by Pauling EN (Excipient's MATS3pe). The relationship among the excipient dose, chemical descriptors, and enhancement rates of absorption are presented in Figures 4–6. Of the plethora of possible combinations, we selected the most significant ones. A 3D plot is given for the relationship among the enhancer's dose, excipient's 9-ordered mean topological charges (JGI9), and ER values calculated according to Equation 5 (Fig. 4).
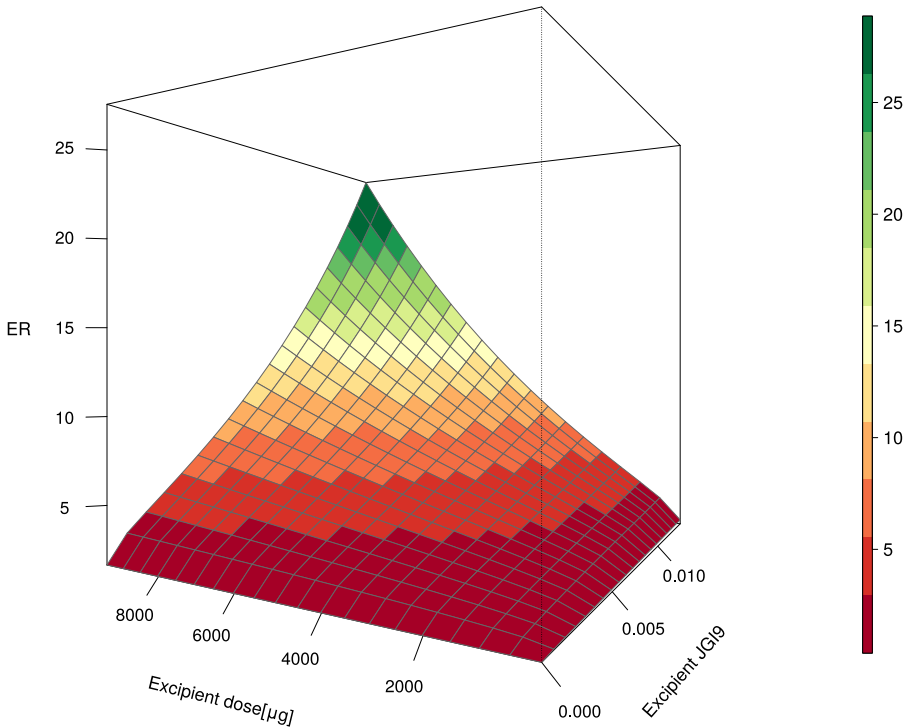

Figure 4. Analysis of influence excipient dose and excipient 9-ordered mean topological charge (JGI9) on enhancement rate predicted by GP model

It can be observed that an increase in the excipient dose generally leads to a marked increase in the ER value. Therefore, the excipient dose has a strong positive impact on the enhancement ratio. At the same time, the positive trend is not as strong

when the enhancer molecule has values of the JGI9 descriptor that are below 0.005. Therefore, the highest increase in the ER is observed for JGI9 descriptors above 0.005 and the enhancer dose above 5000 μg. Such an analysis can lead to the assumption that both the enhancer dose and the topological charge of the excipient (JGI9) can modify the absorption of APIs in the lungs. These findings are in accordance with the work of Li et al. [26], where they studied the influence of the excipient's molecule charge on the liposomes' ability to promote pulmonary protein absorption. Moreover, toxicological studies indicated that the charge of excipients like stearylamine and dicetylphosphate might cause a visible disruption of pulmonary epithelial cells [17]. Furthermore, there is evidence of the relationship among the inhibition of malonyl-CoA decarboxylase activity, the p2x7 receptor, and the topological charge index of the chemical compounds [4, 42]. Galvez's topological charge indices (including JGI9) were also present in the models predicting the Caco2 cell permeability of the chemical compounds [15]. Figure 5 presents a relationship between the enhancers' dose and the APIs' 7-ordered Chi chain-weighted by valence electrons on the enhancement rate calculated according to the GP model (Equation 5).
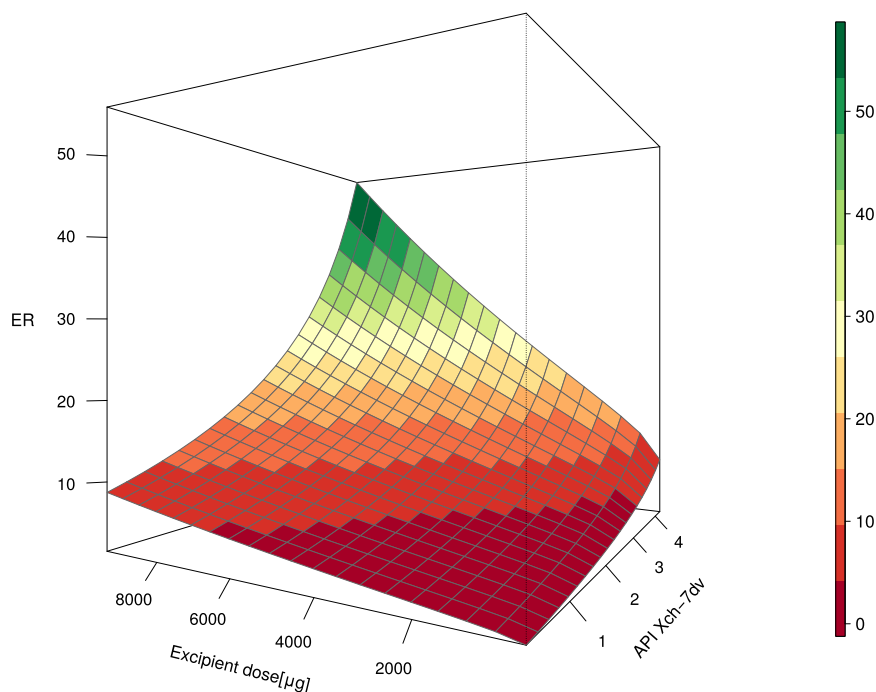

Figure 5. Analysis of influence excipient dose and 7-ordered Chi chain-weighted by valence electrons on enhancement rate predicted by GP model

It can be clearly observed that the absorption enhancement of APIs that have low values of Xch-7dv is not as high as for APIs with Xch-7dv values above 3. An example of such an API is insulin (Xch-7d = 0.34). When Exubera® (the first inhaled insulin)

was marketed in 2006, it was believed that insulin absorption primarily involves a passive diffusion across the alveolar epithelium through extracellular tight junctions [12]. However, the mechanisms of its absorption in the lungs has been questioned recently, providing evidence for transcellular pathways involved in insulin transport across the alveolar epithelial monolayers [48]. Therefore, an in-depth analysis of API molecules may be useful to reveal unknown transportation pathways.

Our findings seem to be in accordance with other research as well. For example, Morita et al. examined the influence of EDTA, salicylate, glycocholate, and caprate on FD4 and FD10 lung absorption [31]. The authors claimed that the absorption of labeled dextrans (FDs) with molecular weights of 4 kDa and 10 kDa (Xch-7dv from 1.9 to 4.2) is highly altered by increasing of the enhancer's dose. They postulated that the observed changes of absorption are related to tight junction structure modifications, causing an increase in paracellular transport. A few years later, Hussain *et al.* classified EDTA and salicylates as tight junction modifiers that act by removing membrane-bound calcium and increasing epithelium permeability [17].
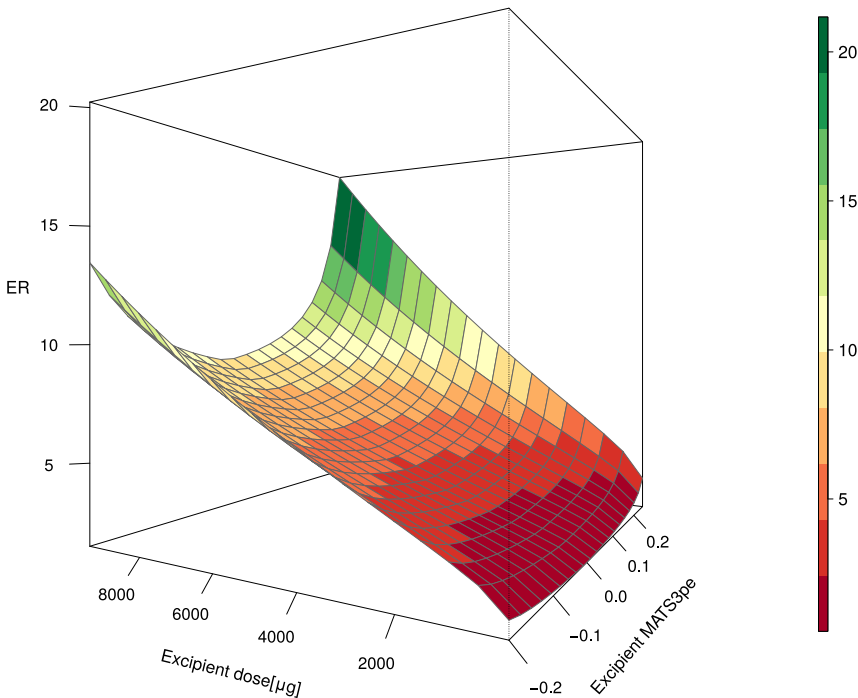

Figure 6. Analysis of influence excipient dose and Moran coefficient of lag 3 weighted by Pauling EN on enhancement rate predicted by GP model

It was found that rhG-CSF's (Xch-7dv = 1.94) absorption in the lungs increases when co-administered with polyethylene glycol (PEG) [17]. Moreover, Okmura *et al.* reported that EDTA and salicylate did not increase insulin (Xch-7d = 0.34) absorption

after lung administration, which can suggest another mechanism of its absorption [35]. EDTA was also ineffective in modifying calcitonin (Xch-7dv = 0.25) absorption in the lungs, suggesting something other than paracellular transport [53].

Figure 6 presents the influence of the enhancer dose and Moran coefficient of lag 3 weighted by Pauling EN (MATS3pe) on the enhancement rate (according to Equation 5). It can be observed that, for negative values of an excipient's MATS3pe, the ER is strongly correlated to the excipient's dose. However, higher ER values are observed for APIs with positive values of MATS3pe.

6. Conclusions

The enhanced and controlled bioavailability of molecules in the lungs plays a crucial role in delivering safe and efficient therapy. Moreover, research on increasing absorption to reduce variability in bioavailability and total patient exposure to APIs and excipients is an ongoing process [48]. However, the development of quality pulmonary formulation regarding particle deposition in the lungs and API absorption is still based on a trial-and-error approach. In this study, an empirical model predicting the influence of absorption enhancers on API bioavailability in the lungs was developed. Starting from a literature review and then encoding chemical compound structures by molecular descriptors, a database was created. Moreover, a feature selection and the construction of predictive models led to a mathematical formula obtained with GP methods. The developed model was analyzed and compared to the empirical results from other research [4, 15, 17, 26, 31, 35, 42, 48, 53]. The presented approach is consistent with recent trends in pharmaceutical technology reflected in regulatory agency guidelines for the industry, which place an emphasis on better understanding the features influencing the final product quality. There is also an acceptance of the FDA for using purely empirical tools as support for medical staff in diagnostics, an example of which is an approved artificial neural network-based diagnostic application – Arterys [6].

The unique approach employed in our work is based on the relative character of the output variable representing the change of two distinct classes of effects: pharmacokinetic and pharmacodynamic. These effects are usually not combined without a PK/PD modeling approach, which integrates both components in the form of differential equations. However, without the results from both components (PK and PD) for a single formulation, it is impossible to establish a classical model. The use of computational intelligence tools allowed us to overcome the necessity of establishing the PK/PD relationship prior to the modeling of drug absorption in the lungs.

References

[1] Agu R.U., Ugwoke M.I., Armand M., Kinget R., Verbeke N.: The lung as a route for systemic delivery of therapeutic proteins and peptides, *Respiratory research*, vol. 2(4), pp. 198–209, 2001. `http://dx.doi.org/10.1186/rr58`.

[2] Al-Tabakha M.M.: Future prospect of insulin inhalation for diabetic patients: The case of Afrezza versus Exubera, *Journal of Controlled Release*, vol. 215, pp. 25–38, 2015. `http://dx.doi.org/10.1016/j.jconrel.2015.07.025`.

[3] Bäckman P., Arora S., Couet W., Forbes B., de Kruijf W., Paudel A.: Advances in experimental and mechanistic computational models to understand pulmonary exposure to inhaled drugs, *European Journal of Pharmaceutical Sciences*, vol. 113, pp. 41–52, 2018. `http://dx.doi.org/10.1016/j.ejps.2017.10.030`.

[4] Banaei A., Pourbasheer E., Haggi F.: QSAR studies and application of genetic algorithm – multiple linear regressions in prediction of novel p2x7 receptor antagonists' activity, *Iranian Chemical Communication*, vol. 4(3), pp. 318–336, 2016. `http://icc.journals.pnu.ac.ir/article_2218.html`.

[5] Bienert S., Waterhouse A., de Beer T., Tauriello G., Studer G., Bordoli L., Schwede T.: The SWISS-MODEL Repository – new features and functionality, *Nucleic Acids Research*, vol. 45(D1), pp. D313–D319, 2017. `http://dx.doi.org/10.1093/nar/gkw1132`.

[6] Bluemke D.A.: Radiology in 2018:Are You Working with AI or Being Replaced by AI? *Radiology*, vol. 287(2), pp. 365–366, 2018. `http://dx.doi.org/10.1148/radiol.2018184007`.

[7] Cannon A.J.: monmlp: Monotone multi-layer perceptron neural network., 2012. `http://cran.r-project.org/web/packages/monmlp/index.html`.

[8] Core R.D.: R: A language and environment for statistical computing. In: *R Foundation for Statistical Computing*, vol. 1, 2008. `https://www.r-project.org`.

[9] Dong Z., Hamid K.A., Gao Y., Lin Y., Katsumi H., Sakane T., Yamamoto A.: Polyamidoamine dendrimers can improve the pulmonary absorption of insulin and calcitonin in rats, *Journal of Pharmaceutical Sciences*, vol. 100(5), pp. 1866–1878, 2011. `http://dx.doi.org/10.1002/jps.22428`.

[10] Edwards C.D., Luscombe C., Eddershaw P., Hessel E.M.: Development of a Novel Quantitative Structure-Activity Relationship Model to Accurately Predict Pulmonary Absorption and Replace Routine Use of the Isolated Perfused Respiring Rat Lung Model, *Pharmaceutical Research*, 33(11), pp. 2604–2616, 2016. `http://dx.doi.org/10.1007/s11095-016-1983-4`.

[11] Eriksson J., Sjögren E., Thörn H., Rubin K., Bäckman P., Lennernäs H.: Pulmonary absorption – estimation of effective pulmonary permeability and tissue retention of ten drugs using an ex vivo rat model and computational analysis, *European Journal of Pharmaceutics and Biopharmaceutics*, vol. 124, pp. 1–12, 2018. `http://dx.doi.org/10.1016/j.ejpb.2017.11.013`.

[12] European Medicines Agency: Scientific discussion in marketing authorisation document for the product EXUBERA, insulin inhalation powder, 2006. `https://www.ema.europa.eu/en/documents/scientific-discussion/exubera-epar-scientific-discussion_en.pdf`.

[13] Flasch O., Mersmann O., Bartz-Beielstein T., Stork J., Zaefferer M.: R genetic programming framework. R package version 0.4-1, 2015. `https://rdrr.io/cran/rgp/`.

[14] Gandomi A.H., Roke D.A.: Assessment of artificial neural network and genetic programming as predictive tools, *Advances in Engineering Software*, vol. 88, pp. 63–72, 2015. `http://dx.doi.org/10.1016/j.advengsoft.2015.05.007`.

[15] Geerts T., Vander Heyden Y.: In silico predictions of ADME-Tox properties: drug absorption, *Combinatorial Chemistry & High Throughput Screening*, vol. 14(5), pp. 339–361, 2011. `http://dx.doi.org/10.2174/138620711795508359`.

[16] He L., Gao Y., Lin Y., Katsumi H., Fujita T., Yamamoto A.: Improvement of pulmonary absorption of insulin and other water-soluble compounds by polyamines in rats, *Journal of Controlled Release*, vol. 122(1), pp. 94–101, 2007. `http://dx.doi.org/10.1016/j.jconrel.2007.06.017`.

[17] Hussain A., Arnold J.J., Khan M.A., Ahsan F.: Absorption enhancers in pulmonary protein delivery, *Journal of Controlled Release*, vol. 94(1), pp. 15–24, 2004 `http://dx.doi.org/10.1016/j.jconrel.2003.10.001`.

[18] Hussain A., Yang T., Zaghloul A.A., Ahsan F.: Pulmonary Absorption of Insulin Mediated by Tetradecyl-β-Maltoside and Dimethyl-β-Cyclodextrin, *Pharmaceutical Research*, vol. 20(10), pp. 1551–1557, 2003. `http://dx.doi.org/10.1023/A:1026118813943`.

[19] Ibrahim M., Garcia-Contreras L.: Mechanisms of absorption and elimination of drugs administered by inhalation, *Therapeutic Delivery*, vol. 4(8), pp. 1027–1045, 2013. `http://dx.doi.org/10.4155/tde.13.67`.

[20] Kerlin R.L., Li X.: Pathology in Non-Clinical Drug Safety Assessment. In: Haschek W.M., Rousseaux C.G., Matthew A. Wallig M.A. (eds.), *Haschek and Rousseaux's Handbook of Toxicologic Pathology*, Chapter 24, pp. 725–750. Academic Press, third ed., 2013. `http://dx.doi.org/10.1016/B978-0-12-415759-0.00024-8`.

[21] Kim S., Thiessen P.A., Bolton E.E., Chen J., Fu G., Gindulyte A., Han L., He J., He S., Shoemaker B.A., Wang J., Yu B., Zhang J., Bryant S.: PubChem Substance and Compound databases: CID 70095, *Nucleic Acids Research*, vol. 44, pp. 1202–1213, 2016. `https://pubchem.ncbi.nlm.nih.gov/`.

[22] Kobayashi S., Kondo S., Juni K.: Pulmonary delivery of salmon calcitonin dry powders containing absorption enhancers in rats, *Pharmaceutical Research*, vol. 13(1), pp. 80–83, 1996. `http://dx.doi.org/10.1023/A:1016081301369`.

[23] Kraljevich T.: h2o: R interface for H20, 2018. `https://cran.r-project.org/package=h2o`.

[24] Kuhn M., Weston S.: Cubist: Rule- And Instance-Based Regression Modeling, 2016. `https://cran.r-project.org/package=Cubist`.

[25] Kumar T.M., Misra A.: Pulmonary absorption enhancement of salmon calcitonin, *Journal of Drug Targeting*, vol. 12(3), pp. 135–144, 2004. `http://dx.doi.org/10.1080/1061186042000223644`.

[26] Li Y., Mitra A.K.: Effects of phospholipid chain length, concentration, charge, and vesicle size on pulmonary insulin absorption, *Pharmaceutical Research*, vol. 13(1), pp. 76–79, 1996. `http://dx.doi.org/10.1023/A:1016029317299`.

[27] Liaw A., Wiener M.: Classification and Regression by RandomForest, *R News*, vol. 2(December), pp. 18–22, 2002. `https://www.r-project.org/doc/Rnews/Rnews_2002-3.pdf`.

[28] Machida M., Hayashi M., Awazu S.: The effects of absorption enhancers on the pulmonary absorption of recombinant human granulocyte colony-stimulating factor (rhG-CSF) in rats, *Biological & Pharmaceutical Bulletin*, vol. 23(1), pp. 84–86, 2000. `http://dx.doi.org/10.1248/bpb.23.84`.

[29] Mitra R., Pezron I., Li Y., Mitra A.K.: Enhanced pulmonary delivery of insulin by lung lavage fluid and phospholipids, *International Journal of Pharmaceutics*, vol. 217(1–2), pp. 25–31, 2001. `http://www.ncbi.nlm.nih.gov/pubmed/11292539`.

[30] Morales J.O., Fathe K.R., Brunaugh A., Ferrati S., Li S., Montenegro-Nicolini M., Mousavikhamene Z., McConville J.T., Prausnitz M.R., Smyth H.D.C.: Challenges and Future Prospects for the Delivery of Biologics: Oral Mucosal, Pulmonary, and Transdermal Routes, *The AAPS Journal*, vol. 19(3), pp. 652–668, 2017. `http://dx.doi.org/10.1208/s12248-017-0054-z`.

[31] Morita T., Yamamoto A., Hashida M., Sezaki H.: Effects of Various Absorption Promoters on Pulmonary Absorption of Drugs with Different Molecular Weights, *Biological & Pharmaceutical Bulletin*, vol. 16(3), pp. 259–262, 1993. `http://dx.doi.org/10.1248/bpb.16.259`.

[32] Moriwaki H., Tian Y.S., Kawashita N., Takagi T.: Mordred: A molecular descriptor calculator, *Journal of Cheminformatics*, vol. 10(1), 2018. `http://dx.doi.org/10.1186/s13321-018-0258-y`.

[33] Nahar K., Gupta N., Gauvin R., Absar S., Patel B., Gupta V., Khademhosseini A., Ahsan F.: *In vitro, in vivo* and *ex vivo* models for studying particle deposition and drug absorption of inhaled pharmaceuticals, *European Journal of Pharmaceutical Sciences*, vol. 49(5), pp. 805–818, 2013. `http://dx.doi.org/10.1016/j.ejps.2013.06.004`.

[34] Nakate T., Yoshida H., Ohike A., Tokunaga Y., Ibuki R., Kawashima Y.: Improvement of pulmonary absorption of cyclopeptide FK224 in rats by coformulating with β-cyclodextrin, *European Journal of Pharmaceutics and Biopharmaceutics*, vol. 55(2), pp. 147–154, 2003. `http://dx.doi.org/10.1016/S0939-6411(02)00158-3`.

[35] Okumura K., Iwakawa S., Yoshida T., Seki T., Komada F.: Intratracheal delivery of insulin Absorption from solution and aerosol by rat lung, *International Journal of Pharmaceutics*, vol. 88(1-3), pp. 63–73, 1992. `http://dx.doi.org/10.1016/0378-5173(92)90304-K`.

[36] Onoue S., Yamamoto K., Kawabata Y., Hirose M., Mizumoto T., Yamada S.: Novel dry powder inhaler formulation of glucagon with addition of citric acid for enhanced pulmonary delivery, *International Journal of Pharmaceutics*, vol. 382(1–2), pp. 144–150, 2009. `http://dx.doi.org/10.1016/j.ijpharm.2009.08.024`.

[37] Pacławski A., Szlęk J., Mendyk A.: Absorption Enhancement Predictor, 2018. `https://sourceforge.net/projects/absorbtionenhancmentpredictor/`.

[38] Pfützner A., Forst T.: Pulmonary insulin delivery by means of the Technosphere™ drug carrier mechanism, *Expert Opinion on Drug Delivery*, vol. 2(6), pp. 1097–1106, 2005. `http://dx.doi.org/10.1517/17425247.2.6.1097`.

[39] Price D.F., Luscombe C.N., Eddershaw P.J., Edwards C.D., Gumbleton M.: The Differential Absorption of a Series of P-Glycoprotein Substrates in Isolated Perfused Lungs from Mdr1a/1b Genetic Knockout Mice can be Attributed to Distinct Physico-Chemical Properties: an Insight into Predicting Transporter-Mediated, Pulmonary Specific Disposition, *Pharmaceutical Research*, vol. 34(12), pp. 2498–2516, 2017. `http://dx.doi.org/10.1007/s11095-017-2220-5`.

[40] Quinlan J.R.: Learning with continuous classes, *Machine Learning*, vol. 92, pp. 343–348, 1992. `http://dx.doi.org/10.1.1.34.885`.

[41] Sanders M.: Inhalation therapy: an historical review, *Primary Care Respiratory Journal: Journal of the General Practice Airways Group*, vol. 16(2), pp. 71–81, 2007. `http://dx.doi.org/10.3132/pcrj.2007.00017`.

[42] Singh P., Kumar R., Sharma B.K., Prabhakar Y.S.: Topological descriptors in modeling malonyl coenzyme A decarboxylase inhibitory activity: *N-Alkyl-N--(1,1,1,3,3,3-hexafluoro-2-hydroxypropylphenyl) amide derivatives*, *Journal of Enzyme Inhibition and Medicinal Chemistry*, vol. 24(1), pp. 77–85, 2009. `http://dx.doi.org/10.1080/14756360801915336`.

[43] Steiner S., Pfützner A., Wilson B.R., Harzer O., Heinemann L., Rave K.: Technosphere/Insulin – proof of concept study with a new insulin formulation for pulmonary delivery, *Exp Clin Endocrinol Diabetes*, vol. 110(1), pp. 17–21, 2002. `http://dx.doi.org/10.1055/s-2002-19989`.

[44] Suarez S., Garcia-Contreras L., Sarubbi D., Flanders E., O'Toole D., Smart J., Hickey A.J.: Facilitation of pulmonary insulin absorption by H-MAP: Pharmacokinetics and pharmacodynamics in rats, *Pharmaceutical Research*, vol. 18(12), pp. 1677–1684, 2001. `http://dx.doi.org/10.1023/A:1013362227548`.

[45] Szlęk J., Pacławski A., Lau R., Jachowicz R., Kazemi P., Mendyk A.: Empirical search for factors affecting mean particle size of PLGA microspheres containing macromolecular drugs, *Computer Methods and Programs in Biomedicine*, vol. 134, pp. 137–147, 2016. `http://dx.doi.org/10.1016/j.cmpb.2016.07.006`.

[46] Szlęk J., Pacławski A., Llau R., Jachowicz R., Mendyk A.: Heuristic modeling of macromolecule release from PLGA microspheres, *International Journal of Nanomedicine*, vol. 8, pp. 4601–4611, 2013. `http://dx.doi.org/10.2147/IJN.S53364`.

[47] Tai L., Li S., Liu M.: Autonomous exploration of mobile robots through deep neural networks, *International Journal of Advanced Robotic Systems*, vol. 14(4), pp. 1–9, 2017. `http://dx.doi.org/10.1177/1729881417703571`.

[48] Takano M., Kawami M., Aoki A., Yumoto R.: Receptor-mediated endocytosis of macromolecules and strategy to enhance their transport in alveolar epithelial cells, *Expert Opinion on Drug Delivery*, vol. 12(5), pp. 813–825, 2015. `http://dx.doi.org/10.1517/17425247.2015.992778`.

[49] Tronde A., Nordén B., Jeppsson A.B., Brunmark P., Nilsson E., Lennernäs H., Bengtsson U.H.: Drug absorption from the isolated perfused rat lung – Correlations with drug physicochemical properties and epithelial permeability, *Journal of Drug Targeting*, vol. 11(1), pp. 61–74, 2003. `http://dx.doi.org/10.1080/1061186031000086117`.

[50] Wang Z.Y., Zhang Q.: Transport of proteins and peptides across human cultured alveolar A549 cell monolayers, *International Journal of Pharmaceutics*, vol. 269(52), pp. 451–456, 2004. `http://dx.doi.org/10.1016/j.ijpharm.2003.09.033`.

[51] Wiśniowska B., Mendyk A., Szlek J., Kołaczkowski M., Polak S.: Enhanced QSAR models for drug-triggered inhibition of the main cardiac ion currents, *Journal of Applied Toxicology*, vol. 35(9), pp. 1030–1039, 2015. `http://dx.doi.org/10.1002/jat.3095`.

[52] Yamamoto A., Fujita T., Muranishi S.: Pulmonary absorption enhancement of peptides by absorption enhancers and protease inhibitors, *Journal of Controlled Release*, vol. 41(1–2), pp. 57–67, 1996. `http://dx.doi.org/10.1016/0168-3659(96)01480-0`.

[53] Yamamoto A., Okumura S., Fukuda Y., Fukui M., Takahashi K., Muranishi S.: Improvement of the Pulmonary Absorption of (Asu[1,7])-Eel Calcitonin by Various Absorption Enhancers and Their Pulmonary Toxicity in Rats, *Journal of Pharmaceutical Sciences*, vol. 86(10), pp. 1144–1147, 1997. `http://dx.doi.org/10.1021/js9603764`.

Affiliations

Adam Pacławski [ID]

Jagiellonian University Medical College, Department of Pharmaceutical Technology and Biopharmaceutics, ul. Medyczna 9, 30-688 Krakow, Poland, e-mail:adam.paclawski@uj.edu.pl, ORCID ID: https://orcid.org/0000-0003-2801-6197

Jakub Szlęk [ID]

Jagiellonian University Medical College, Department of Pharmaceutical Technology and Biopharmaceutics, ul. Medyczna 9, 30-688 Krakow, Poland, ORCID ID: https://orcid.org/0000-0003-1537-9650

Aleksander Mendyk [ID]

Jagiellonian University Medical College, Department of Pharmaceutical Technology and Biopharmaceutics, ul. Medyczna 9, 30-688 Krakow, Poland, ORCID ID: https://orcid.org/0000-0002-4394-9115